

# THz BASED PHASE-SPACE MANIPULATION IN A GUIDED IFEL\*

E. Curry<sup>†</sup>, S. Fabbri, P. Musumeci, UCLA, Los Angeles, CA 90049, USA  
 A. Gover, Tel-Aviv University, Tel-Aviv 69978, Israel

## Abstract

We propose a guided IFEL interaction driven by a broadband THz source to compress a relativistic electron bunch and synchronize it with an external laser pulse. A high field single-cycle THz pulse is group velocity-matched to the electron bunch inside a waveguide, allowing for a sustained interaction in a magnetic undulator. The THz pulse is generated via optical rectification from the external laser source, with a measured peak field of up to 4.6 MV/m. We present measurements of the THz waveform before and after a parallel plate waveguide with varying aperture size and estimate the group velocity. We also present results from a preliminary 1-D multi-frequency simulation code we are developing to model the guided broadband IFEL interaction. Given a 6 MeV, 100 fs electron bunch with an initial  $10^{-3}$  energy spread, as can be readily produced at the UCLA PEGASUS laboratory, the simulations predict a phase space rotation of the bunch distribution that will reduce the initial timing jitter and compress the electron bunch by nearly an order of magnitude.

## INTRODUCTION

As the development of THz sources pushes towards higher power, the pursuit of THz applications in accelerator physics has become an active field of research. In addition to the unique advantages of THz radiation for imaging and spectroscopy [1], the THz frequency range offers a middle ground in beam manipulation between the high-acceleration-gradient of laser wavelengths and the broad phase-acceptance window of RF. The transverse kick imparted to an electron bunch in an X-band RF deflector, like the one used for temporal diagnostics at LCLS [2], could be accomplished by a THz field that is over fifty times smaller. The higher frequency of THz relative to RF may also allow for improvement of the breakdown limitations in an accelerating structure [3]. Where laser coupling in a typical FEL results in microbunching of the electron beam, an FEL interaction with THz radiation could capture and compress the entire bunch within a single ponderomotive bucket.

At the UCLA PEGASUS laboratory, we intend to demonstrate the compression of a 1 pC electron bunch using ponderomotive coupling with a THz pulse. A single Ti:Sapph laser source will be used to generate THz through optical rectification while simultaneously driving a 1.6 cell S-band photogun. The ponderomotive force produced by the THz and undulator fields gives the electron bunch an energy chirp, resulting in longitudinal compression after a drift section.

The THz pulse is synchronized with the external laser pulse. When the phase of the ponderomotive bucket is centered on the average arrival time of the electron bunches, the induced energy chirp works to accelerate late bunches and decelerate early bunches towards the optimal timing, compensating for the inherent time-of-arrival jitter that accrues over the course of the initial electron bunch acceleration.

## ZERO-SLIPPAGE IFEL

The resonance condition of a standard inverse free electron laser (IFEL) assumes slippage between the electron bunch and the laser waveform to maintain a phase synchronism condition as they propagate in free-space. For the single-cycle THz pulse produced by optical rectification, an interaction can be sustained by satisfying a "zero-slippage" condition, or grazing dispersion curve condition, in which the THz group velocity is matched to the average longitudinal speed of the electron bunch [4][5], in addition to satisfying the phase synchronism condition. This velocity-matching occurs when the dispersion curves for the waveguide and electron beam, shown in Fig. 1, have the same slopes. The control of THz pulse group velocity can be accomplished by a waveguide. This technique has the added benefit of preserving the on-axis field intensity over the length of the guide rather than operating in the diffraction limited regime.

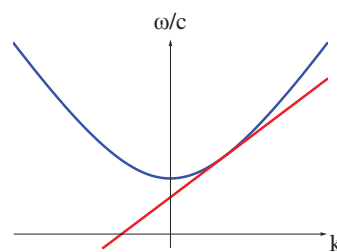


Figure 1: The dispersion curves for a waveguide (blue) and electron beam (red). The "zero-slippage" condition occurs when their slopes, corresponding to radiation group velocity and average longitudinal bunch velocity, are equal.

The THz frequency range is an ideal candidate for this guided IFEL technique. Although higher frequencies can offer a larger acceleration gradient, the size of the guiding structures becomes prohibitively difficult for co-propagation of electrons and laser. The length scales necessary for a THz guiding structure are large enough to permit alignment of the electron beam and accommodate the oscillating trajectory of the electrons in an IFEL without clipping. For reasonably low charge, wakefield effects in the guiding structure are negligible.

\* Work supported by DOE grant DE-FG02-92ER40693 and NSF grant PHY-1415583.

<sup>†</sup> e Curry@physics.ucla.edu

The IFEL-type phase-space manipulation we have proposed relies on ponderomotive coupling with the transverse field in the guide. Given excitation of the appropriate mode, a guiding structure can also provide a longitudinal field for direct coupling to the electron beam. This method of acceleration has been successfully demonstrated in ref. [6] for low energy electrons. However, for relativistic electrons, like those generated at PEGASUS laboratory, ponderomotive coupling is more efficient [7].

## THz SOURCE CHARACTERIZATION

We use optical rectification in stoichiometric lithium niobate (sLN) to generate picosecond scale THz pulses. To enhance the conversion efficiency from IR to THz, the pulse front of the IR laser is tilted using a diffraction grating and imaged onto the sLN with a focusing lens [8][9]. With .1% conversion efficiency, we have  $1.2 \mu\text{J}$  pulses with a peak field of  $3 \text{ MV/m}$  after the diverging THz pulse is collimated and focused by a pair off-axis parabolic mirrors (OAP). By increasing the laser spotsize along with laser power, we can stay below the sLN damage threshold. Using  $2.3 \text{ mJ}$  of IR power, we produce a peak field of  $4.6 \text{ MV/m}$ , shown in Fig. 2b. We are developing a cooling chamber to further improve the conversion efficiency at the sLN crystal. With this modification, we can expect the peak field to increase by at least a factor of two [10].

Measurements of the temporal field profile are conducted with electro-optic sampling (EOS) in .5 mm thick zinc telluride. Within this nonlinear optical crystal, a THz induced rotation of the fast and slow axes changes the relative intensity between the horizontal and vertical polarization components of an IR probe pulse. A balanced detection scheme utilizes a quarter waveplate and Wollaston prism to separate these components onto two photodiodes. The original THz field is then calculated in terms of the intensity difference [11].

The IR probe pulse is brought into collinear propagation with the THz using a pellicle that is transparent to THz. For measurements of the THz profile after the waveguide, the IR probe travels within the guide, before interacting with the THz in the ZnTe crystal placed at the exit. The relatively high-frequency probe pulse is undistorted in the guide.

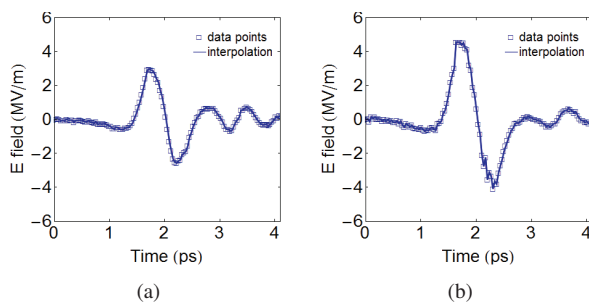


Figure 2: THz profile with (a) undoubled spot size and (b) doubled spot size.

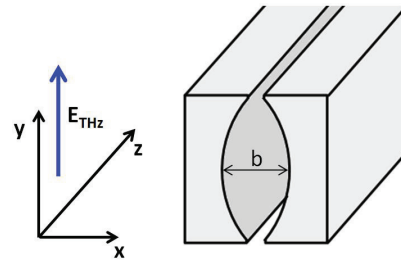


Figure 3: Diagram showing cross section of PPWG, with plate spacing  $b$ , and the orientation of THz polarization to excite the  $TE_{01}$  mode.

## GUIDED THz PROPAGATION

We have adopted the curved parallel plate waveguide (PPWG) to control the propagation of the THz pulse. This choice was inspired by the investigation of guiding structures for a THz FEL oscillator in ref. [12] and [13]. The PPWG structure, shown in Fig. 3, offers the unique advantage of variable plate spacing which allows for tuning of the guide's dispersive properties and the corresponding group velocity of the THz pulse. Using an OAP, we focus the THz pulse into the entrance of the PPWG. This direct coupling of the THz pulse, with a gaussian transverse profile, excites the  $TE_{01}$  mode in the PPWG [14].

In Fig. 4, we show the THz longitudinal pulse profile after a 20 cm PPWG for three different plate spacings. The pulse profile before the waveguide is shown in Fig. 2a. The plates were machined from aluminum with a 3 mm radius of curvature. Because the plate alignment was set by eye, we list the plate spacings as nominally "3.5 mm," "2.5 mm," and "1.5 mm" in accordance with caliper measurements taken at both ends. Shown on the right in Fig. 4 are predicted pulse profiles based on the entering profile and the dispersion relation of the  $TE_{01}$  mode for the particular plate spacing. In the "1.5 mm" plate spacing measurement, the PPWG reached the limit at which the plate edges touched, resulting in some changes to the plates' alignment.

The group velocity of the THz pulse within the PPWG can be estimated by comparing the IR probe delay between the peak field in the initial and final THz pulse profile. After the "1.5 mm" plate spacing, the delay between the entering and exiting peak field was 4.03 ps, giving  $\beta_g = .9940$ . After the "2.5 mm" plate spacing, the delay was 2.47 ps, giving  $\beta_g = .9963$ . The delay for the THz pulse propagating in the "3.5 mm" plate spacing shown in Fig. 4 could not be determined because of backlash in the translation stage between measurements. However, a THz pulse generated by an IR pulse with doubled spotsize experienced a delay of 1.62 ps after the same "3.5 mm" spacing, giving  $\beta_g = .9976$ . The theoretical group velocities of .84 THz, the peak frequency of the pulse, for the three plate spacings are .9903 at 1.5 mm spacing, .9962 at 2.5 mm spacing, and .9979 at 3.5 mm spacing. The discrepancies between the measured and expected delays are most likely the result of plate misalignment, as well as plate contact for the case of the "1.5 mm" spacing.

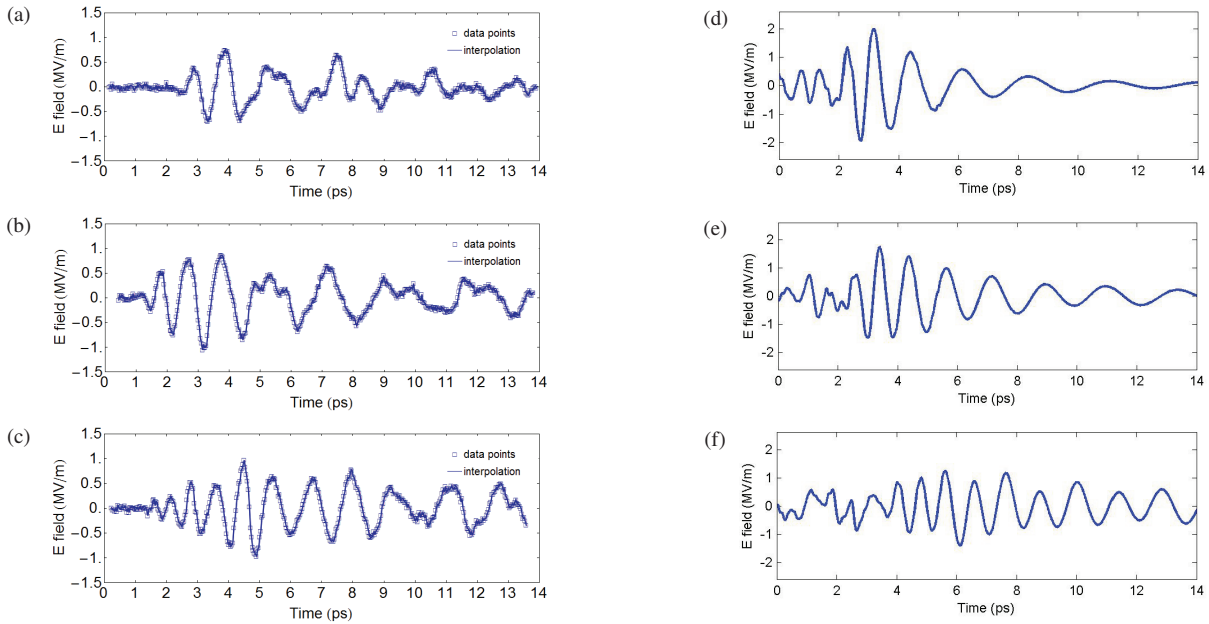


Figure 4: On the left, EOS measurements of the THz profile after a 20 cm PPWG with a plate spacing of (a) "3.5 mm," (b) "2.5 mm," and (c) "1.5 mm." On the right, predicted THz profile after the PPWG with plate spacing (d) "3.5 mm," (e) "2.5 mm," and (f) "1.5 mm," based on the THz profile measured at the entrance of the PPWG and shown in Fig. 2a.

### SIMULATION STUDIES

Ponderomotive coupling with a single cycle THz pulse cannot be well-described by the single frequency approximation used by most FEL simulation codes because of the broad spectral content of the THz pulse. We are currently developing a multi-frequency simulation code, similar to MUFFIN [15], which will track the evolution of the THz pulse spectrum. The calculation does not rely on the slowly varying envelop approximation or period averaging and includes the waveguide-induced dispersion of the THz pulse.

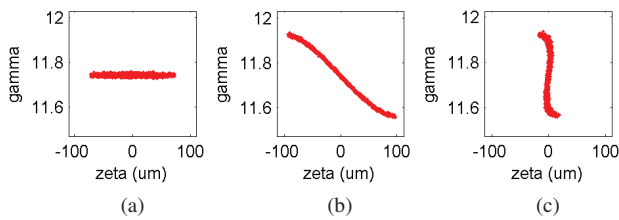


Figure 5: Simulation results showing the longitudinal phase space distribution (a) before the undulator, (b) at the exit of the undulator, and (c) after a .7 m drift period.

Preliminary simulation results are shown in Fig. 5, with the corresponding simulation parameters in Table 1. These waveguide parameters were chosen for the simulation because at the peak frequency they correspond to a theoretical group velocity of  $\beta_g = .994$  which we have already experimentally achieved using the "1.5 mm" plate spacing. The selected electron bunch parameters are well within the range that can be routinely generated at PEGASUS laboratory [16] [17]. The sample 100 fs electron bunch, shown

in Fig. 5, is compressed to 12.5 fs, almost an order of magnitude, after a .7 m drift. Given a timing jitter as great as 100 fs, the ponderomotive interaction cuts the timing jitter down to 40 fs while still compressing the bunch by a factor of 3.

Table 1: Simulation Parameters

Bunch energy	6 MeV
Energy spread	$10^{-3}$
Bunch length	100 fs rms
Undulator period	3 cm
Undulator parameter, K	1.32
# of undulator periods	8
PPWG spacing, b	2.06 mm
Plate curvature radius	2 mm
Peak THz field	10 MV/ m
Peak frequency	.84 THz
FWHM of spectrum	2.35 THz
# of frequency points	51
Frozen field approximation	On

### CONCLUSION

To efficiently harness the power of a single cycle THz pulse for beam manipulation, the problem of extending the interaction time must be solved. Towards achieving a sustained interaction, we have demonstrated tunable control of the group velocity of a THz pulse inside a PPWG. Using velocity matching between the THz pulse and an electron bunch, we will sustain a "zero-slippage" IFEL interaction

to both compress the electron bunch and reduce its time-of-arrival jitter. Based on the 1-D multifrequency simulation code that we are currently developing, we should achieve up to an order of magnitude of bunch compression. Looking forward, the "zero-slippage" interaction that we will demonstrate in the PPWG can be extended to a transverse deflection mechanism, like the one proposed in ref. [18], without the need for an additional RF deflecting cavity to resolve the THz streaking.

### ACKNOWLEDGMENT

We are grateful for the support of the U.S. Department of Energy through grant DE-FG02-92ER40693 and the National Science Foundation through grant PHY-1415583.

### REFERENCES

- [1] P.U. Jepsen, D.G. Cooke, and M. Koch. In: *Laser and Photonics Reviews* 5.1 (2011), pp. 124–166. ISSN: 1863-8899.
- [2] C Behrens et al. In: *Nature communications* 5 (2014).
- [3] A. Hassanein et al. In: *Physical Review Special Topics-Accelerators and Beams* 9 (6 2006), p. 062001.
- [4] A Doria, GP Gallerano, and A Renieri. In: *Optics communications* 80.5 (1991), pp. 417–424.
- [5] A. Gover et al. In: *Physical review letters* 72 (8 1994), pp. 1192–1195.
- [6] E.A. Nanni et al. In: *preprint arXiv:1411.4709* (2014).
- [7] A. Gover et al. *Encyclopedia of Modern Optics*. 2005. <http://www.eng.tau.ac.il/research/FEL/Encyclopedia%20of%20Modern%20Optics1.pdf>
- [8] A.G. Stepanov, J. Hebling, and J. Kuhl. In: *Applied physics letters* 83.15 (2003), pp. 3000–3002.
- [9] J Hebling et al. In: *Applied Physics B* 78.5 (2004), pp. 593–599.
- [10] B. Bartal et al. English. In: *Applied Physics B* 86.3 (2007), pp. 419–423. ISSN: 0946-2171.
- [11] M. Brunken et al. DESY, 2003.
- [12] I.M. Yakover, Y. Pinhasi, and A. Gover. In: *Nuclear Instruments and Methods in Physics Research Section A: Accelerators, Spectrometers, Detectors and Associated Equipment* 375.1 (1996), pp. 260–263.
- [13] I.M. Yakover, Y. Pinhasi, and A. Gover. In: *Nuclear Instruments and Methods in Physics Research Section A: Accelerators, Spectrometers, Detectors and Associated Equipment* 358.1 (1995), pp. 323–326.
- [14] Rajind Mendis and Daniel M Mittleman. In: *Journal of the Optical Society of America B* 26.9 (2009), A6–A13.
- [15] N. Piovella. In: *Physics of Plasmas (1994-present)* 6.8 (1999), pp. 3358–3368.
- [16] P Musumeci et al. In: *Physical review letters* 100.24 (2008), p. 244801.
- [17] J. T. Moody et al. In: *Physical Review Special Topics-Accelerators and Beams* 12 (7 2009), p. 070704.
- [18] G. Andonian et al. In: *Physical Review Special Topics-Accelerators and Beams* 14.7 (2011), p. 072802.